Thermal conductivity of solid argon at high pressure and high temperature: A molecular dynamics study

Konstantin V. Tretiakov
The Abdus Salam International Centre for Theoretical Physics (ICTP), Strada Costiera 11, I-34100 Trieste, Italy and Institute of Molecular Physics, Polish Academy of Sciences, Smoluchowskiego 17/19, 60-179 Poznań, Poland

Sandro Scandolo
The Abdus Salam International Centre for Theoretical Physics (ICTP), Strada Costiera 11, I-34100 Trieste, Italy and INFM/Democritos National Simulation Center, I-34100 Trieste, Italy

(Received 13 July 2003; accepted 13 September 2004)

The thermal conductivity of solid argon at high-pressure (up to 50 GPa) and high-temperature (up to 2000 K) has been calculated by equilibrium molecular dynamics simulations using the Green–Kubo formalism and an exponential-6 interatomic potential. A simple empirical expression is given for its pressure and temperature dependence. The results are compared with predictions based on kinetic theory. The relative change of the thermal conductivity λ with density ρ is found to be consistent with a $\partial \ln \lambda / \partial \ln \rho$ slope of approximately 6 in a wide range of pressures and temperatures, in good agreement with predictions based on kinetic theory.
 [DOI: 10.1063/1.1812754]

I. INTRODUCTION

Argon is extensively used as a pressure transmitting medium in high-pressure and high-temperature diamond-anvil cell (DAC) experiments, because its softness prevents the development of large pressure gradients in the sample.[1,2] Temperature gradients are more difficult to control, as the high thermal conductivity of diamond in the anvils forces temperature to drop in a few microns from the desired value in the sample (typically a few thousand kelvins) down to ambient temperature at the anvil surface. The thermal conductivity of the pressure transmitting medium is a crucial parameter in heat-transfer calculations aimed at determining the temperature distribution inside the cell.[1,3] In the case of argon, the thermal conductivity has been measured[4–6] at ambient pressure up to the melting point, but its pressure dependence has never been examined from an experimental standpoint, despite the fact that the pressure dependence of the thermal conductivity is known to have a stronger influence on temperature gradient calculations than its temperature dependence.[7] Heat-transfer calculations of the temperature gradient in a DAC are presently based on simple scaling models for the pressure and temperature dependence of the thermal conductivity of solid argon.[1]

At variance with scaling models, which are typically based on kinetic theory and on the existence of a single characteristic time for phonon scattering in solids, molecular dynamics (MD) provides in principle an exact description of the dynamical properties of solids, including thermal conductivity, without any further assumption other than the form of the potential of interaction between atoms. Atomic interactions in argon are extremely well described by simple pair potentials, of the Lennard-Jones form at low pressure, and of the so-called exponential-6 form at high pressure. We have recently calculated the temperature dependence of the thermal conductivity of solid Ar at ambient pressure,[8] using MD and the Lennard-Jones potential, and found it to be within 20% of the experimental values. Motivated by the success of MD in reproducing the thermal conductivity λ of solid argon at ambient pressure, we now extend the calculation of λ using MD, to finite pressures, up to 50 GPa.

The paper has two main purposes. On one hand, we aim at providing DAC modelers with an accurate theroretical prediction of the P-T dependence of the thermal conductivity of argon, one of the most common pressure transmitting media. To this aim, we will present a simple formula for $\lambda(P,T)$, which we hope will be of practical use in DAC modeling. On the other hand, we would like to check and verify the validity of simple scaling laws based on kinetic theory in estimating pressure effects on λ. We find that scaling of λ with density is reasonably well reproduced by kinetic theory but that scaling laws provide only an order-of-magnitude estimate of pressure effects on λ.

The paper is organized as follows: In Sec. II we describe the method of calculation and present the simulation details. In Sec. III we show how we calculate the quantities needed to determine the thermal conductivity from kinetic theory. In Sec. IV we discuss the MD results for the thermal conductivity and compare them with those obtained from kinetic theory. Section V contains summary and conclusions.

II. METHOD

Argon is a rare gas solid and a wide-gap insulator, so we can safely assume that the electronic contribution to the thermal conductivity is negligible, and focus our analysis on the lattice contribution only. Radiative heat tranfer is also believed to be irrelevant up to at least 3000 K.[1] At the temperatures of interest for this study (>150 K) quantum effects on the nuclei are negligible and the atomic dynamics can be

considered as purely classical. Like most other condensed rare gases, the atomic dynamics of argon is described with very good accuracy by simple pair potentials. For pressure up to 1 GPa, interactions are accurately described by a Lennard-Jones (LJ) potential[9]

$$\phi(r_{ij}) = 4\epsilon\left[\left(\frac{\sigma}{r_{ij}}\right)^{12} - \left(\frac{\sigma}{r_{ij}}\right)^{6}\right], \tag{1}$$

where r_{ij} is the distance between atoms i and j. The values of the parameters ϵ and σ that best reproduce the thermodynamics of Ar at ambient pressure are $\epsilon/k_B = 119.8$ K and $\sigma = 3.405$ Å, where k_B is the Boltzmann constant.[10] We used the LJ potential for all calculations at ambient pressure. At high pressure, however, the exponential-6 (Exp-6) pair potential of Ross and co-workers[11,12] is known to yield a better description of the equation of state. The Exp-6 potential is given by

$$\phi(r_{ij}) = \left(\frac{\epsilon}{\alpha - 6}\right)\left\{6\exp\left[\alpha\left(1 - \frac{r_{ij}}{\sigma}\right)\right] - \alpha\left(\frac{\sigma}{r_{ij}}\right)^{6}\right\} \tag{2}$$

with parameters $\epsilon/k_B = 122$ K, $\sigma = 3.85$ Å, and $\alpha = 13$ based on high-pressure shock-wave data up to 40 GPa.[11] We used the Exp-6 potential in all calculations at finite pressure ($P > 1$ GPa).

We calculate λ using the Green–Kubo formula:[10]

$$\lambda = \frac{1}{3Vk_BT^2}\int_0^\infty \langle \mathbf{j}(0)\cdot\mathbf{j}(t)\rangle dt, \tag{3}$$

where V is the volume, T the temperature, and the angular brackets denote the ensemble average, or, in the case of a MD simulation, the average over initial conditions. The microscopic heat current is given by

$$\mathbf{j}(t) = \sum_i \mathbf{v}_i\varepsilon_i + \frac{1}{2}\sum_{i,j,i\neq j}\mathbf{r}_{ij}(\mathbf{F}_{ij}\cdot\mathbf{v}_i), \tag{4}$$

where $\mathbf{v}_i$ is the velocity of particle i, $\mathbf{F}_{ij}$ is the force on atom i due to its neighbor j from the pair potential (1) or (2). The ''local'' energy ε_i is given by

$$\varepsilon_i = \frac{1}{2}m_i\mathbf{v}_i^2 + \frac{1}{2}\sum_j \phi(\mathbf{r}_{ij}), \tag{5}$$

where m is the mass of atom.

MD simulations were performed in the N-V-T ensemble where temperature was controlled via a Nosé-Hoover (NH) thermostat.[13] The fourth-order Runge–Kutta integration scheme was used to integrate the equations of motion. In order to avoid problems related to unwanted noncanonical fluctuations of the instantaneous temperature in NH thermostatted simulations (the so-called ''Toda demon''), we follow the prescriptions of Ref. 14.

Simulation details for LJ calculations are identical to those of Ref. 8. For Exp-6 calculations the integration time step Δt was set to 0.001τ (the Exp-6 unit of time is $\tau = \sqrt{m\cdot\sigma^2/\epsilon}$, or 2.42 ps for argon). The typical lengths of the runs were equal to 5×10^5 MD steps, after equilibration (10^5 MD steps). Longer runs (5×10^6 MD steps) were also performed to check the convergence of the results on simulation time. The Exp-6 pair potential was cut off at a radius of 2.5σ, or at $(L/2)\sigma$ (where L is the size of the simulation box) in case the latter was smaller than 2.5σ. Long-range corrections to the energy are given by[15]

$$U_{LRC} = 2\pi\rho\int_{R_c}^\infty \phi(r)r^2dr, \tag{6}$$

where $\phi(r)$ is the interatomic pair potential, ρ is the density of system, and R_c is the cutoff radius. For the Exp-6 potential we obtain

$$U_{LRC} = \frac{2\pi\rho\epsilon}{\alpha-6}\left(\frac{6e^{\alpha(1-R_c)}[1+(1+\alpha R_c)^2]}{\alpha^3} - \frac{\alpha}{3R_c^3}\right), \tag{7}$$

while long-range energy corrections for the LJ potential are discussed in Ref. 15. Simulations were performed with cubic cells containing of $N = 256$ particles [solid argon crystallizes in the face-centered cubic (fcc) lattice, with four atoms in the conventional cubic cell]. Periodic boundary conditions were imposed in all three directions. As shown in Ref. 8, the size dependence of the thermal conductivity calculated with the Green–Kubo formula is weak. Calculations with $N = 108$ particles were shown to be sufficiently large to make size effect negligible at ambient pressure. At high pressure however the size of the box with $N = 108$ particles would be smaller than 2σ, so we found that results were fully converged in simulation size only with $N = 256$ particles.

The thermal conductivity was calculated by discretizing the right-hand side of Eq. (3) in MD time steps Δt as

$$\lambda = \frac{\Delta t}{3Vk_BT^2}\sum_{m=1}^{M}\frac{1}{(N-M)}\sum_{n=1}^{N-m}\mathbf{j}(m+n)\mathbf{j}(n), \tag{8}$$

where N is the number of MD steps after equilibration, M is the number of steps over which the time average is calculated, and $\mathbf{j}(m+n)$ is the heat current at MD time step $m+n$. M was set to $(1-2)\times10^4$, which is considerably smaller than the number of MD steps, in order to ensure good statistical averaging.

In order to check the numerical accuracy of the Green–Kubo (GK) method, we show in Fig. 1 the time evolution of typical heat autocorrelation functions at different pressures, together with their time integrals, Eq. (3).

III. KINETIC THEORY

Thermal conductivities obtained from MD simulations will be compared in the following section with the predictions of kinetic theory, so we briefly describe here how we obtain λ from kinetic theory. The thermal conductivity can be written, in kinetic theory, as

$$\lambda = \frac{1}{3}C_V v l, \tag{9}$$

where C_V is the specific heat per unit volume, v is the average velocity of sound in the solid, and l is the mean free path of the energy-carrying particle. In solids, where lattice vibrations are described in terms of phonons, l is limited, at high temperature, by phonon-phonon scattering, and can be estimated as[16]

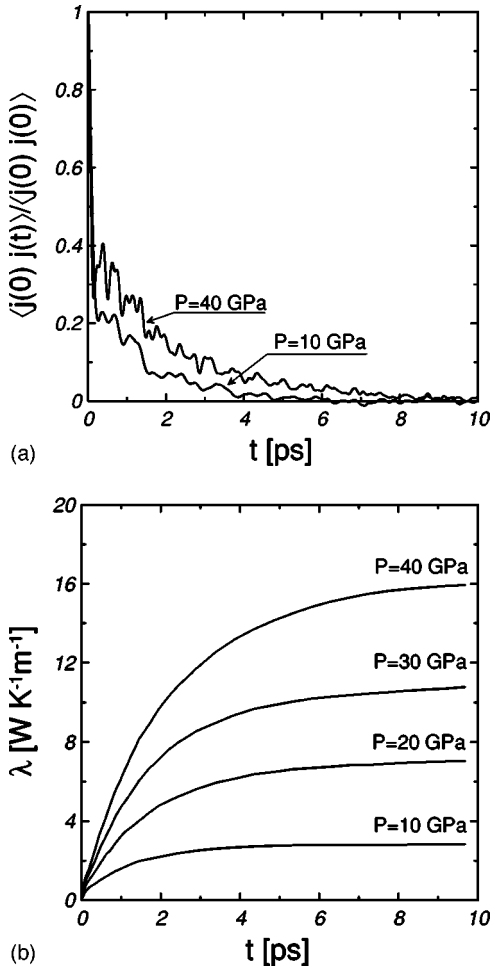

FIG. 1. Time dependencies at $T=400$ K and different pressures of (a) heat autocorrelation function and (b) thermal conductivity.

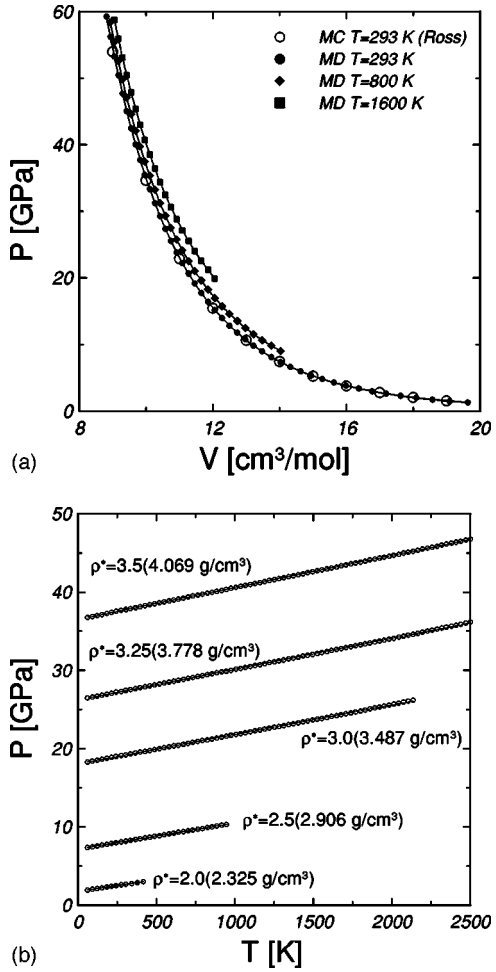

FIG. 2. Equations of state of solid argon at high pressure. (a) Volume dependence of pressure at different temperatures. Solid symbols are present work. Open circles are the results of Ross *et al.* (Ref. 12). (b) Temperature dependence of pressure at different densities. Densities are expressed both in reduced units and real units ($\rho^*=\rho\sigma^3/m$).

$$l \simeq \frac{d}{\alpha\gamma T}, \tag{10}$$

where d is the interatomic distance, α is the thermal expansion coefficient, γ is the thermodynamic Grüneisen parameter. The calculation of λ from kinetic theory therefore requires the calculation of C_V, v, α, and γ at the pressure and temperature conditions of interest.

C_V was fixed to the value for the classical harmonic solid ($C_V=3Nk_B/V$) which was found to approximate very well the actual value computed by differentiating the internal energy at a few P-T points. In order to determine the bulk modulus, the Grüneisen parameter and the coefficient of thermal expansion, we calculated with MD the equations of state (V-P and P-T) of solid argon at different temperatures and densities, respectively (Fig. 2). At room temperature our results [Fig. 2(a)] compare very well with those of Ross *et al.*[12] (as they should, since the pair potential used in 12 is identical to the one used here). The isothermal bulk modulus $[B=-V(\partial P/\partial V)_T]$ obtained from the equation of state compares well with experimental data[17,18] [Fig. 3(a)], even though the agreement becomes poorer at the highest pressures (50 GPa). This is reasonable, since the Exp-6 potential was created and tested for pressures only up to 40 GPa.[11,12] The coefficient of thermal expansion was determined from[19]

$$\alpha = \frac{1}{B}\left(\frac{\partial P}{\partial T}\right)_V. \tag{11}$$

In Fig. 2(b) we show the temperature dependence of the pressure at different densities, which turns out to be linear at all densities. The partial derivative in Eq. (11) was then easily obtained from the results of Fig. 2(b) and its volume dependence is presented in Fig. 3(b). The volume dependence of the thermal expansion coefficient is shown in Fig. 4(a). The Grüneisen parameter was obtained as[19]

$$\gamma = \frac{\alpha B}{C_V}, \tag{12}$$

and its volume dependence is shown in Fig. 4(b). The results are in good agreement with previous calculations.[12]

We finally describe the calculation of the average sound velocity v. The average sound velocity is given, in Debye theory, by[20]

$$v = \left[\frac{1}{3}\left(\frac{1}{v_L^3}+\frac{2}{v_T^3}\right)\right]^{-1/3}, \tag{13}$$

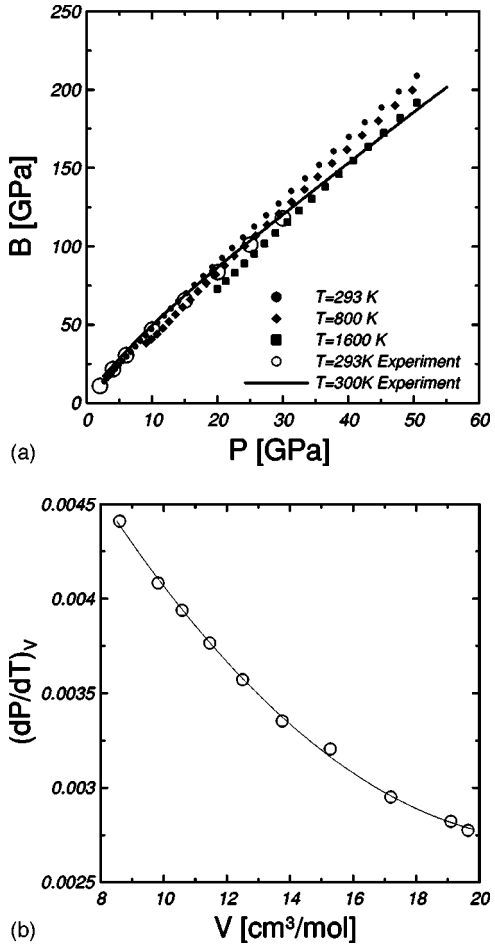

FIG. 3. (a) Pressure dependence of the bulk modulus at different temperatures. Solid symbols are present work. Open circles are experimental results of Grimsditch *et al.* (Ref. 17). The solid line is the experimental result of Shimizu *et al.* (Ref. 18). (b) Volume dependence of the temperature derivative of pressure. Open circles are the results of MD simulation. Solid line is the fit to simulation data.

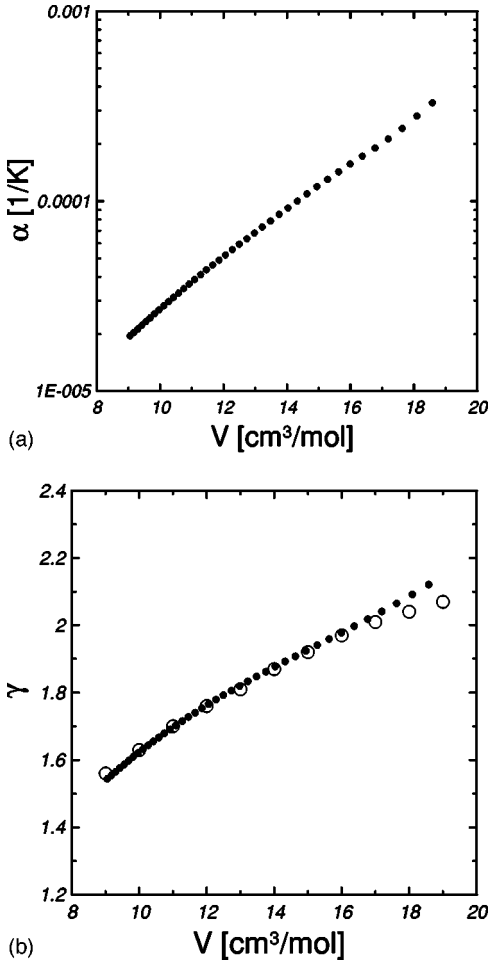

FIG. 4. (a) Volume dependence of the thermal expansion coefficient. (b) Volume dependence of the thermodynamic Grüneisen parameter. Dots are present work. Open circles are the results of Ross *et al.* (Ref. 12).

where v_L and v_T are longitudinal and transverse average sound velocities. For a cubic lattice v_L and v_T coincide with the longitudinal and transverse velocities along the (100) direction.[18,20] Assuming that the phonon frequencies of solid Ar are well described by a nearest-neighbor interaction model, then the frequencies of the longitudinal and of the transverse mode are[21]

$$\omega_L(k)=\omega_{LO}\sin\frac{ka}{4},\quad \omega_T(k)=\omega_{TO}\sin\frac{ka}{4}, \tag{14}$$

where $\omega_{LO}=4v_L/a$ and $\omega_{TO}=4v_T/a$. Phonon frequencies ω_{LO} and ω_{TO} were calculated from the peaks of the Fourier transform of the velocity autocorrelation functions at $\mathbf{k}=(2\pi/a,0,0)$, along the three Cartesian directions $(\alpha=x,y,z)$:[10]

$$C^{\alpha}(\omega)\simeq\int_{-\infty}^{\infty}\exp(i\omega t)\langle v^{\alpha}(t)v^{\alpha}(0)\rangle dt, \tag{15}$$

with

$$v^{\alpha}=\sum_i v_i^{\alpha}e^{-i\mathbf{k}\cdot\mathbf{r}_i}, \tag{16}$$

$\mathbf{r}_i$ being the position of atom i and v_i^{α} the α Cartesian component of its velocity.

In Fig. 5(a) we compare our results for the longitudinal and transverse velocities along (100) with available experimental data[18] and find that the agreement is excellent. Figure 5(b) shows the volume dependence of the average sound velocity calculated using Eq. (13).

IV. RESULTS AND DISCUSSION

Pressure and temperature dependencies of the thermal conductivity of solid argon obtained with the GK method are presented in Fig. 6. The temperature dependence [Fig. 6(a)] deviates slightly from the T^{-1} law, and is better represented by a $T^{-\beta}$ law, with β varying between 1.2 to 1.5. The same behavior was observed at ambient pressure both in experiment and simulation.[8] The linear dependence of λ with pressure in the log-log plot of Fig. 6(b) suggests a power law also for the dependence of λ on pressure. Based on these observations, we fitted our high-pressure GK results to a simple empirical expression where the logarithms of both temperature and pressure appear lineraly. A best-fit analysis of the data of Fig. 6 gives

$$\log(\lambda)=2.6-1.31\log(T)+1.29\log(P), \tag{17}$$

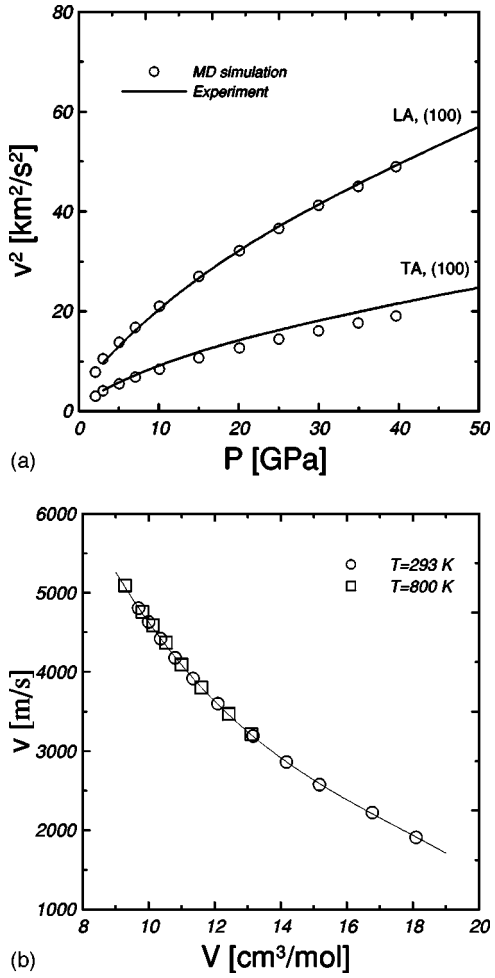

FIG. 5. (a) Pressure dependence of the square of the longitudinal and transverse velocities. Open circles are present work. The lines are experimental results of Shimizu *et al.* (Ref. 18). (b) Volume dependence of the average sound velocity. Line is the fit to the data.

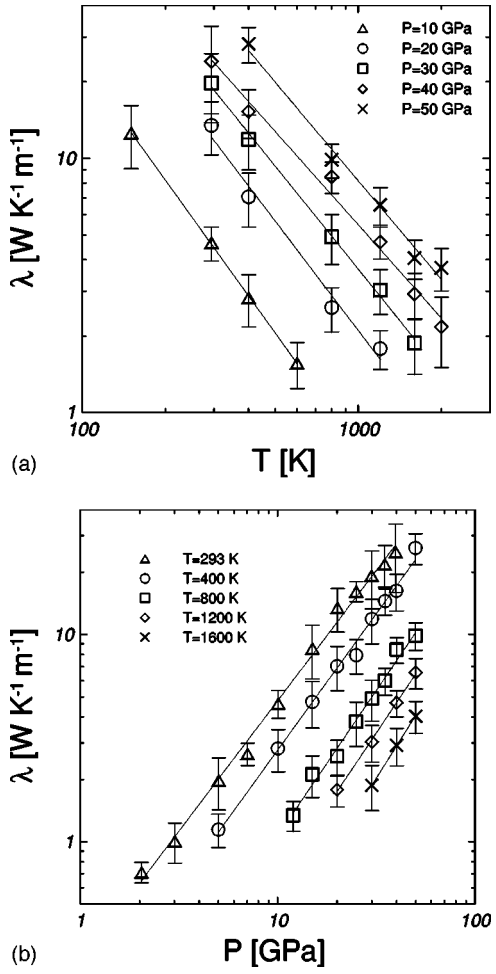

FIG. 6. (a) Temperature dependence of the thermal conductivity of solid argon at different pressures. (b) Pressure dependence of the thermal conductivity at different temperatures.

where λ is in W/K m, P is in GPa, and T in Kelvin. Figure 6(a) shows how well the empirical expression (17) reproduces the simulation data. The range of validity of expression (17) is limited to the range $2 \leqslant P \leqslant 50$ GPa and $150 \leqslant T \leqslant 2000$ K and to the domain of stability of the solid phase.

The density dependence of λ calculated with the GK method is shown in Fig. 7(b), where it is compared with the results obtained from kinetic theory (KT). Kinetic theory systematically overestimates the GK results, by an amount ranging from 1.5–2 times at ambient pressure (see Table I), up to a factor 4 at high pressure. At ambient pressure, where comparison with experimental data is available, the GK results agree within less than 20% with experiments, while the results of KT overestimate the experimental results by about 25–50%. KT is known to overestimate the thermal conductivity in a number of other systems.[16] This is probably a consequence of an overestimation of the phonon mean free path as given by Eq. (10). GK and KT, however, give a similar scaling of the thermal conductivity with density. Linear fits to the curves shown in Fig. 7(b) result in slopes of about 6 ± 0.3, with marginally higher slopes for KT. Such slopes compare very well with the the scaling expression[19,23]

$$\left(\frac{\partial \ln \lambda}{\partial \ln \rho}\right)_T \approx \frac{\partial \ln B}{\partial \ln \rho} - 2\frac{\partial \ln \gamma}{\partial \ln \rho} + \frac{\partial \ln v}{\partial \ln \rho} - \frac{1}{3} \tag{18}$$

obtained from KT (dimensional analysis shows that in the expression published in Ref. 19 the term $-4/3$ should be replaced by $-1/3$).[24] Density averaged values for the above quantities, as obtained by linear fitting of the data presented in the previous section, yield, for example at room temperature, $\partial \ln B/\partial \ln \rho = 4.25$, $\partial \ln \gamma/\partial \ln \rho = -0.42$, and $\partial \ln v/\partial \ln \rho = 1.4$, which result, using Eq. (18), in a slope of 6.2, in nice agreement with the slopes of Fig. 6(b).

TABLE I. Comparison of the thermal conductivity at ambient pressure obtained in the present work using LJ potential (λ_{GK}, λ_{KT}) with experimental data (Ref. 4) and with an independent theoretical determination (Ref. 22). Temperatures and densities (T and ρ) are expressed in K and g/cm^3. Thermal conductivities are in W/K m. The values of $T = 25$ and 75 K were extrapolated from McGaughey's data (Ref. 22).

T	ρ	λ_{GK}	λ_{GK} (Ref. 22)	λ_{expt} (Ref. 4)	λ_{KT}
25	1.784	1.14(19)	1.120	1.43	2.22
50	1.721	0.43(6)	0.417	0.549	0.755
75	1.647	0.23(3)	0.230	0.255	0.321

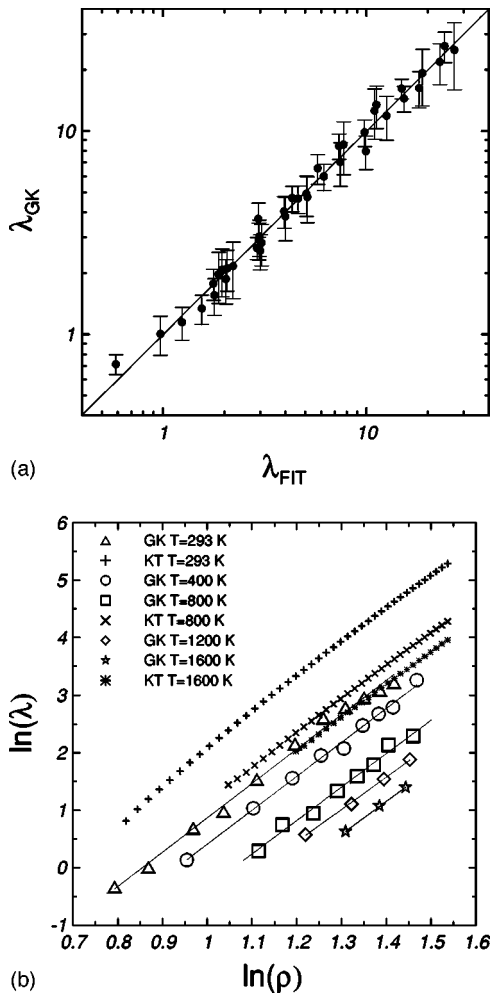

FIG. 7. (a) Comparison between the values of the thermal conductivity determined by the Green–Kubo method with those obtained using the empirical expression (17). (b) Density dependence of the thermal conductivity of solid argon at different temperatures.

V. CONCLUSIONS

Based on molecular dynamics simulations we have determined the pressure and temperature dependence of the thermal conductivity of solid argon in the pressure range $2<P<50$ GPa and in the temperature range $150<T<2000$ K. We provide a simple empirical expression [Eq. (17)] which we hope will be of practical use in modeling thermal gradients in diamond-anvil cells when argon is used as the pressure-transmitting medium.

We also verified that kinetic theory can be safely used for qualitative predictions of pressure effects on the thermal conductivity, but we found that the discrepancy between kinetic theory and simulations increases with pressure and temperature.

ACKNOWLEDGMENTS

We acknowledge useful discussions with Tom Duffy, Boris Kiefer, Roberto Car, Krzysztof Wojciechowski, David Heyes, William Hoover, and Young-Gui Yoon. S.S. acknowledges partial support from NSF/CSEDI. Part of this work was supported by Grant No. 4T11F01023 of the Polish Committee for Scientific Research (KBN).

[1] A. Dewaele, G. Fiquet, and Ph. Gillet, Rev. Sci. Instrum. **69**, 2421 (1998).
[2] Y. Meng, D. J. Weidner, and Y. Fei, Geophys. Res. Lett. **20**, 1147 (1993).
[3] W. R. Panero and R. Jeanloz, J. Geophys. Res. **106**, 6493 (2001).
[4] I. N. Krupskii and V. G. Manzhelii, Sov. Phys. JETP **28**, 1097 (1969).
[5] F. Clayton and D. N. Batchelder, J. Phys. C **6**, 1213 (1973).
[6] D. K. Christensen and G. L. Pollack, Phys. Rev. B **12**, 3380 (1975).
[7] M. Manga and R. Jeanloz, Geophys. Res. Lett. **23**, 1845 (1996).
[8] K. V. Tretiakov and S. Scandolo, J. Chem. Phys. **120**, 3765 (2004).
[9] Y. Choi, T. Ree, and F. H. Ree, Phys. Rev. B **48**, 2988 (1993).
[10] M. P. Allen and D. J. Tildesley, *Computer Simulation of Liquids* (Clarendon, Oxford, 1987).
[11] M. Ross, J. Chem. Phys. **73**, 4445 (1980).
[12] M. Ross, H. K. Mao, P. M. Bell, and J. A. Xu, J. Chem. Phys. **85**, 1028 (1986).
[13] D. Frenkel and B. Smit, *Understanding Molecular Simulation* (Academic, San Diego, 2002).
[14] B. L. Holian, A. F. Voter, and R. Ravelo, Phys. Rev. E **52**, 2338 (1995).
[15] D. M. Heyes, *The Liquid State Application of Molecular Simulation* (Wiley, Chichester, 1998).
[16] J. S. Dugdale and D. K. MacDonald, Phys. Rev. **98**, 1751 (1955).
[17] M. Grimsditch, P. Loubeyre, and A. Polian, Phys. Rev. B **33**, 7192 (1986).
[18] H. Shimizu, H. Tashiro, T. Kume, and S. Sasaki, Phys. Rev. Lett. **86**, 4568 (2001).
[19] D. L. Anderson, *Theory of the Earth* (Blackwell, Boston, 1989).
[20] J-P. Poirier, *Introduction to the Physics of Earth's Interior* (Cambridge University Press, Cambridge, 1991).
[21] N. W. Ashcroft and N. D. Mermin, *Solid State Physics* (Saunders, Philadelphia, 1976).
[22] A. J. H. McGaughey and M. Kaviany, Int. J. Heat Mass Transfer **47**, 1783 (2004).
[23] M. Manga and R. Jeanloz, J. Geophys. Res. **102**, 2999 (1997).
[24] D. L. Anderson and R. Jeanloz (private communication).